

# Calexcitin B Is a New Member of the Sarcoplasmic Calcium-binding Protein Family\*

Received for publication, November 20, 2000, and in revised form, March 30, 2001  
Published, JBC Papers in Press, April 16, 2001, DOI 10.1074/jbc.M010508200

Zoltan Gombos<sup>‡§</sup>, Andreas Jeromin<sup>¶||</sup>, Tapas K. Mal<sup>‡\*\*</sup>, Avijit Chakrabartty<sup>‡</sup>,  
and Mitsuhiro Ikura<sup>‡‡</sup>

From the <sup>‡</sup>Division of Molecular and Structural Biology, Ontario Cancer Institute and Department of Medical Biophysics, University of Toronto, Toronto, Ontario M5G 2M9, Canada and the <sup>¶</sup>Institute of Medical Science, University of Toronto and Samuel Lunenfeld Research Institute, Mount Sinai Hospital, Toronto, Ontario M5G 1X5, Canada

Calexcitin (CE) is a calcium sensor protein that has been implicated in associative learning. The CE gene was previously cloned from the long-finned squid, *Loligo pealei*, and the gene product was shown to bind GTP and modulate K<sup>+</sup> channels and ryanodine receptors in a Ca<sup>2+</sup>-dependent manner. We cloned a new gene from *L. pealei*, which encodes a CE-like protein, here named calexcitin B (CE<sub>B</sub>). CE<sub>B</sub> has 95% amino acid identity to the original form. Our sequence analyses indicate that CEs are homologous to the sarcoplasmic calcium-binding protein subfamily of the EF-hand superfamily. Far and near UV circular dichroism and nuclear magnetic resonance studies demonstrate that CE<sub>B</sub> binds Ca<sup>2+</sup> and undergoes a conformational change. CE<sub>B</sub> is phosphorylated by protein kinase C, but not by casein kinase II. CE<sub>B</sub> does not bind GTP. Western blot experiments using polyclonal antibodies generated against CE<sub>B</sub> showed that CE<sub>B</sub> is expressed in the *L. pealei* optic lobe. Taken together, the neuronal protein CE represents the first example of a Ca<sup>2+</sup> sensor in the sarcoplasmic calcium-binding protein family.

Calcium ions (Ca<sup>2+</sup>) play a vital role in cells, being involved in various signaling events from cell growth to cell death. Many Ca<sup>2+</sup>-dependent cellular processes are mediated by Ca<sup>2+</sup>-binding proteins (CaBPs),<sup>1</sup> which share a common Ca<sup>2+</sup> binding

motif, termed “EF-hand” (1). EF-hand proteins can be subdivided into two types. A “Ca<sup>2+</sup> sensor” regulates downstream target proteins in a Ca<sup>2+</sup>-dependent manner and a “Ca<sup>2+</sup> buffer” contributes to maintaining the intracellular Ca<sup>2+</sup> level (2). Calmodulin, troponin C, S100 proteins, frequenin, and neurocalcin are examples of Ca<sup>2+</sup> sensors, whereas sarcoplasmic calcium-binding proteins (SCPs), parvalbumin, and calbindin D<sub>9k</sub> are thought to function as Ca<sup>2+</sup> buffers (2).

Recently, a new CaBP called calexcitin (CE) has been identified in squid and implicated to play a role in associative learning through inhibition of K<sup>+</sup> channels in a Ca<sup>2+</sup>-dependent manner (3–5). Subsequently, it was reported (6) that CE binds and activates ryanodine receptors, which are also involved in associative learning (7). CE has been shown to possess GTP binding and GTPase activities (4), but its functional significance is unknown. The gene encoding CE was cloned, and the recombinant protein was shown to bind Ca<sup>2+</sup> and to be a high affinity substrate for protein kinase C (PKC) (4). To date, in addition to ryanodine receptor activation (6) and K<sup>+</sup> channel inhibition (4), a number of other functions have been proposed for CE, including an involvement in the pathophysiology of Alzheimer’s disease (8, 9), induction of mRNA turnover (5), and transformation of inhibitory postsynaptic potentials to excitatory postsynaptic potentials (10). Although the mechanisms underlying these multiple functions are not well understood, most of the proposed functions appear to be mediated by Ca<sup>2+</sup> (5).

In this paper, we describe a new homologue of CE, termed CE<sub>B</sub> (the original form of CE (Ref. 4) is denoted CE<sub>A</sub> for clarity). This new gene differs in nucleotide sequence from the CE<sub>A</sub> gene, containing an insertion near its 3’ end, leading to a longer open reading frame. Our sequence analyses indicate that CEs are members of the SCP subfamily of the EF-hand superfamily. The recombinant CE<sub>B</sub> has been expressed and purified from *Escherichia coli* and characterized using biochemical and biophysical techniques.

## EXPERIMENTAL PROCEDURES

**Gene Cloning**—Primers were based on the DNA sequence of CE<sub>A</sub> (accession no. U49390) (4). The sense primer (SP) had an *Nde*I site and the sequence gggaaattccatagggctgccatcaactttccgatttcc. The antisense primer (AP1) had a *Bam*HI site and the sequence cgggatccgttttagggtaacaaacagatgggtgcc. Polymerase chain reaction was used, and the template was *Loligo pealei* optic lobe cDNA with *Eco*RI adapters (provided by Dr. J. Battey, National Institutes of Health, Bethesda, MD). Since a nucleotide addition was always observed near the 3’ end of the amplified product, the antisense primer was changed based on the CE<sub>A</sub> sequence (4), to allow the amplification of a product with an extended 3’

*latum* muscle SCP isoform; DTT, dithiothreitol; MES, 4-morpholineethanesulfonic acid.

\* This work was supported by a grant from the Canadian Institutes of Health Research (to A. C. and M. I.). The costs of publication of this article were defrayed in part by the payment of page charges. This article must therefore be hereby marked “advertisement” in accordance with 18 U.S.C. Section 1734 solely to indicate this fact.

The nucleotide sequence(s) reported in this paper has been submitted to the GenBank™/EBI Data Bank with accession number(s) AF322410.

§ Supported by a Natural Sciences and Engineering Research Council postgraduate scholarship award, a Savoy Foundation for Epilepsy Studentship, and a Canadian Institutes of Health Research doctoral research award.

|| Supported by a Canadian Institutes of Health Research doctoral research award.

\*\* Supported by an Ontario Cancer Institute/Amgen postdoctoral fellowship and a National Cancer Institute of Canada research fellowship.

‡‡ Recipient of Canadian Institutes of Health Research scientist award and Howard Hughes Medical Institute international scholar award. To whom correspondence should be addressed: Ontario Cancer Inst., Rm. 7-723, 610 University Ave., Toronto, Ontario M5G 2M9, Canada. Tel.: 416-946-2025; Fax: 416-946-6529; E-mail: mikura@uhres.utoronto.ca.

<sup>1</sup> The abbreviations used are: CaBP, calcium-binding protein; CD, circular dichroism; CE, calexcitin; CKII, casein kinase II; HSQC, heteronuclear single-quantum correlation; PKC, protein kinase C; SCP, sarcoplasmic calcium-binding protein; PAGE, polyacrylamide gel electrophoresis; SP, sense primer; AP, antisense primer; ASCP, *B. lanceo-*

sequence and the sequence cgggacctctaaagtgtttgggtaccaacagatgg. SP and the new antisense primer (AP2) were used to amplify CE<sub>B</sub> using polymerase chain reaction and the cDNA template described above. CE<sub>B</sub> was cloned into a modified pGEX-2TK vector (Amersham Pharmacia Biotech, Baie d'Urfe, Quebec, Canada), which had a *Nde*I site (pGEX-2TK-*Nde*I; provided by P. Yin, University of Toronto, Ontario, Canada), and sequenced. The deduced amino acid sequence was aligned with ClustalX (11). Since the homology in some regions within the sequence alignment was low, the secondary structure assignment of the *Branchiostoma lanceolatum* SCP (ASCP) (12) was used to manually adjust residues in loop regions.

**Protein Expression and Purification**—*E. coli* BL21 cells transformed with pGEX-2TK-*Nde*I-CE<sub>B</sub> were grown at 37 °C. The glutathione *S*-transferase-CE<sub>B</sub> fusion protein was induced with 1 mM isopropyl β-D-thiogalactoside and after 3 h, cells were centrifuged, resuspended in 10 mM Tris-HCl (pH 7.5), 10 mM dithiothreitol (DTT), 1 mM EDTA, 2 Complete tablets (Roche Molecular Biochemicals, Laval, Quebec, Canada), and stored at -20 °C. Upon thawing, cells were kept on ice, sonicated, and incubated with 1% Triton X-100 for 30 min. The solution was centrifuged and the soluble fraction incubated overnight at 4 °C with glutathione-Sepharose 4B (Amersham Pharmacia Biotech) with gentle shaking. The beads containing the bound fusion protein were washed with phosphate-buffered saline solution (13) at 4 °C and then washed with 50 mM Tris-HCl (pH 8), 150 mM NaCl, 0.1% 2-mercaptoethanol, 2.5 mM CaCl<sub>2</sub> at room temperature. CE<sub>B</sub> was cleaved from glutathione *S*-transferase by incubation with 50 units of thrombin (Calbiochem, San Diego, CA) overnight at room temperature. To the eluted protein, 1 mM phenylmethylsulfonyl fluoride and 10 mM CaCl<sub>2</sub> were added, checked for purity by sodium dodecyl sulfate-polyacrylamide gel electrophoresis (SDS-PAGE), and stored at 4 °C. The CE<sub>B</sub> N-terminal sequence was analyzed by Edman degradation (University of British Columbia, Vancouver, British Columbia, Canada) and its weight measured by electron-spray mass spectrometry (University of Waterloo, Waterloo, Ontario, Canada). Both of these confirmed the identity of CE<sub>B</sub>.

**Ca<sup>2+</sup> Overlay Blot**—CE<sub>B</sub> was run on SDS-PAGE and transferred onto nitrocellulose (Bio-Rad, Mississauga, Ontario, Canada). The overlay blot was performed as described previously (14). After the blot was dried, it was subjected to phosphorimaging (Storm 840) and analyzed by ImageQuant software (Amersham Pharmacia Biotech).

**Western Blot Hybridization**—Polyclonal anti-CE<sub>B</sub> antibodies were prepared in rabbits with full-length CE<sub>B</sub> as the antigen. The antibodies were affinity-purified on CNBr-activated Sepharose 4B (Amersham Pharmacia Biotech) containing CE<sub>B</sub>. CE<sub>B</sub> and *L. pealei* optic lobe (provided by Drs. D. L. Alkon and T. J. Nelson, National Institutes of Health, Bethesda, MD) were run on SDS-PAGE, blotted onto nitrocellulose, and blocked with skim milk. The blot was incubated for 3 h with a 10,000-fold dilution of anti-CE<sub>B</sub> antibodies, washed, and incubated for 3 h with a 3,000-fold dilution of horseradish peroxidase-conjugated goat anti-rabbit IgG antibodies (Bio-Rad). Following extensive washing, the blot was exposed using ECL chemiluminescence (Amersham Pharmacia Biotech).

**Protein Kinase C (PKC) and Casein Kinase II (CKII) Phosphorylation**—CE<sub>B</sub> (~2 μg) was added either to 20 mM Tris-HCl (pH 8), 0.5 mM CaCl<sub>2</sub>, 100 μg/ml phosphatidylserine (Avanti, Alabaster, AL), 20 μg/ml diacylglycerol (Avanti), 10 mM MgCl<sub>2</sub>, 1% bovine serum albumin, 0.1 units of PKC (Pierce), and 125 Ci/liter [ $\gamma$ -<sup>32</sup>P]ATP (A) or to 4 mM MES (pH 6.9), 25 mM KCl, 2 mM MgCl<sub>2</sub>, 1 mM DTT, 0.020 milliunits CKII (Roche Molecular Biochemicals), and 50 Ci/liter [ $\gamma$ -<sup>32</sup>P]ATP (B). Solutions were incubated at 37 °C for 1 h, run on SDS-PAGE, and subjected to autoradiography, as described above. To check the stoichiometry of PKC phosphorylation, the above reaction (A) was repeated with the substitution of [ $\gamma$ -<sup>32</sup>P]ATP to 10 μM ATP and the molecular weight of the sample measured by electron-spray mass spectrometry (University of Waterloo, Waterloo, Ontario, Canada). To determine the effect of PKC phosphorylation on the conformation of CE<sub>B</sub>, the above reaction was repeated at large scale using 25 μg of CE<sub>B</sub> and 1.25 units of PKC (Pierce). The control sample contained all the components of the phosphorylated sample with the exception of ATP. Following incubation, the samples and buffers were passed through a Centricon YM30 spin column (Millipore, Bedford, MA) followed by a PD-10 column (Amersham Pharmacia Biotech). The protein concentrations in both phosphorylated and unphosphorylated samples were found to be identical using UV absorption. Under denaturing conditions in 6 M guanidine-HCl and using an extinction coefficient of  $\epsilon_{280} = 49270 \text{ M}^{-1} \text{ cm}^{-1}$ , calculated by the method of Gill and von Hippel (15), the protein concentration in these samples were found to be 5 μM. These samples were used in the circular dichroism and fluorescence experiments described below.

**Circular Dichroism (CD) Spectroscopy**—CD measurements were made on an Aviv 62DS spectropolarimeter at room temperature. To study the effect of Ca<sup>2+</sup> on the conformation of CE<sub>B</sub>, the protein was prepared by dialyzing against a solution containing 1 mM MES (pH 7). Samples were made with either 1 mM CaCl<sub>2</sub> (A) or 1 mM EGTA (B). Far UV spectra were recorded in a 0.1-cm quartz cuvette. The protein solution was 169 μg/ml, as determined by UV absorption and described above. The data were deconvoluted using the CD Spectra Deconvolution program (version 2.1; provided by Dr. G. Böhm, Martin-Luther-Universität, Halle-Wittenberg, Germany). Near UV spectra were recorded in a 1-cm quartz cuvette with a protein solution of 2.3 mg/ml (determined by UV absorption as described above). The CD parameters used for the phosphorylation experiment were identical to those described above for the Ca<sup>2+</sup> binding experiment.

**Fluorescence Spectroscopy**—Steady-state fluorescence was measured using a Photon Technology International QM-1 spectrofluorometer equipped with excitation intensity correction. Emission spectra were collected from 305 to 400 nm ( $\lambda_{\text{ex}} = 295 \text{ nm}$ , 1 s/nm, band pass = 2 nm for excitation and emission). For the Ca<sup>2+</sup> binding experiments, samples were decalcified through dialysis in the presence of EGTA followed by dialysis against decalcified water. CE<sub>B</sub> was diluted to a final concentration of about 50 μM (as determined by UV absorption and described above) in 100 mM KCl and 50 mM HEPES (pH 7.5). Sample volumes were 0.5 ml, and experiments were performed at 27 °C. The Ca<sup>2+</sup> titration curve to calculate the Ca<sup>2+</sup> dissociation constant ( $K_d$ ) was generated in the presence of 1.5 mM EGTA with the sequential addition of 0.2 mM CaCl<sub>2</sub>. The emission spectrum was collected after each CaCl<sub>2</sub> addition. Then, the fluorescence intensities from 305 to 400 nm were integrated. The free Ca<sup>2+</sup> concentration was calculated based on the total amounts of Ca<sup>2+</sup> and EGTA present using a web-based computer algorithm (MAXCHELATOR). The Ca<sup>2+</sup> binding curve used to calculate the number of Ca<sup>2+</sup> binding sites was generated with the sequential addition of a 10 mM CaCl<sub>2</sub> stock (0.25–1 μl) until saturation and then with a 100 mM CaCl<sub>2</sub> stock (0.5 μl). Sample dilution was never more than 1.5%. The parameters used in the fluorescence spectroscopy for the phosphorylation experiment were identical to those described above for the Ca<sup>2+</sup> binding experiment with the exception of the band pass, which was set to 1 nm for both excitation and emission.

**Two-dimensional Nuclear Magnetic Resonance (NMR) Spectroscopy**—Uniformly <sup>15</sup>N-labeled CE<sub>B</sub> was expressed in M9 medium (13) containing <sup>15</sup>NH<sub>4</sub>Cl and purified as described above. CE<sub>B</sub> was dialyzed against either a solution containing 10 mM Tris-HCl (pH 7.5), 1 mM DTT, and 10 mM CaCl<sub>2</sub> (A) or a solution containing 10 mM Tris-HCl (pH 7.5), 1 mM DTT, and 10 mM EGTA (B). NMR sample concentration was about 1 mM <sup>15</sup>N-labeled CE<sub>B</sub> in 5% <sup>2</sup>H<sub>2</sub>O. The protein concentration in the Ca<sup>2+</sup>-bound and Ca<sup>2+</sup>-free (apo) samples was identical. The Ca<sup>2+</sup>-GTP and apo-GTP samples were prepared by the addition of 2 mM GTP to the Ca<sup>2+</sup> and apo samples, respectively. The protein concentration in the Ca<sup>2+</sup>-GTP and apo-GTP samples was also identical and was only 0.2% less than the original (Ca<sup>2+</sup> and apo) samples, due to the addition of GTP. NMR spectra were acquired at 37 °C on a Varian Unity-Plus 500 spectrometer. Two-dimensional <sup>15</sup>N-<sup>1</sup>H heteronuclear single-quantum correlation (HSQC) spectra (16, 17) were recorded using the enhanced sensitivity method (18), with 16 transients and 128 and 512 complex points in the <sup>15</sup>N (F<sub>1</sub>) and <sup>1</sup>H (F<sub>2</sub>) dimensions, respectively.

## RESULTS

The nucleotide sequence of the *L. pealei* CE<sub>B</sub> (Fig. 1A) is 99% identical to that of CE<sub>A</sub>, with the major difference being a single nucleotide insertion near the 3' end of the sequence. The deduced amino acid sequence of CE<sub>B</sub> (Fig. 1B) shows 95% identity to CE<sub>A</sub> (4). Another homologous protein (here referred to as CE<sub>T</sub>; accession no. AF078951) from the Japanese common squid, *Todarodes pacificus*, has been identified through a BLAST search. CE<sub>T</sub> shows 93% amino acid identity to CE<sub>B</sub> (Fig. 1B). Moreover, we found that CE<sub>B</sub> shows 28% amino acid identity to ASCP (19), which is higher than the identity score (15–20%) reported among various members of the SCP subfamily (20). CE<sub>B</sub> also shows 45% amino acid identity to a neuronal SCP from *Drosophila melanogaster* (dSCP2) and 18% identity to a muscle SCP from *D. melanogaster* (21) (dSCP1; Fig. 1B). CE<sub>B</sub> also shares 34% (F56D1.6, accession no. Q10131) and 28% (T09A5.1, accession no. P54961) amino acid identity to putative proteins predicted from the *Caenorhabditis elegans* genome (22) (Fig. 1B).



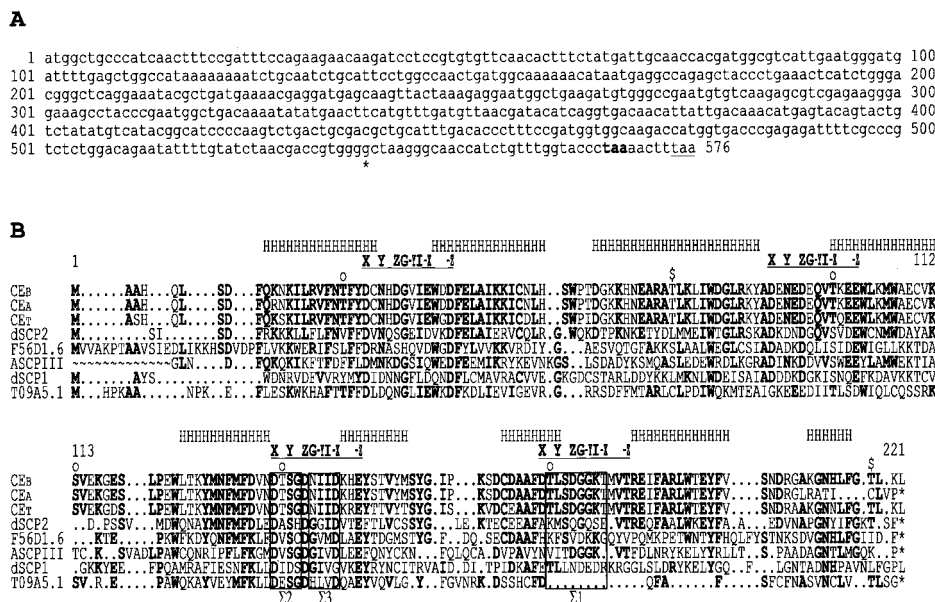


FIG. 1. Nucleotide and deduced amino acid sequence of CE<sub>B</sub>. A, nucleotide sequence of the full-length CE<sub>B</sub> cDNA. Nucleotide numbers are indicated, and the stop codon is underlined. The stop codon of CE<sub>A</sub> is indicated in bold and the major nucleotide difference between CE<sub>B</sub> and CE<sub>A</sub> is marked by an asterisk (\*). B, the deduced amino acid sequence of CE<sub>B</sub> is aligned with CE<sub>A</sub> (4), calexcitin from *T. pacificus* (CE<sub>T</sub>), the *D. melanogaster* neuronal dSCP2 (21), a putative *C. elegans* neuronal homologue (F56D1.6) (22), a *B. lanceolatum* muscle SCP isoform (ASCP III) (19), the *D. melanogaster* muscle dSCP1 (21), and a putative *C. elegans* muscle homologue (T09A5.1) (22). Amino acids are numbered on top, and significant residue identities are shown in bold. The helices found in ASCP are indicated on the top of the alignment (H). ASCP contains only short  $\beta$  sheet regions, holding pairs of EF-hands together in the Ca<sup>2+</sup> binding loop areas (12) (these have not been indicated). A line indicates the proposed Ca<sup>2+</sup> binding loop in putative EF-hands. X, Y, Z, -X, and -Z indicate potential residues involved in Ca<sup>2+</sup> coordination, which typically are residues containing oxygen in their side chains (Asn, Asp, Gln, Glu, Ser, and Thr) (24). -Y indicates the sixth potential residue involved in Ca<sup>2+</sup> coordination. G indicates the sixth residue within the loop region, which is predominantly Gly in typical EF-hands, and I indicates the residue that is Ile, Leu, or Val in the canonical EF-hand (24). Potential CKII (o) and PKC (\$) phosphorylation sites are shown, as determined by PROSITE. CE<sub>B</sub> differs by one amino acid from the deduced amino acid sequence of a gene deposited to GenBank by Nelson *et al.* (accession no. AAC32271; position 11 is Lys in CE<sub>B</sub> and Arg in AAC32271). This Lys residue has been confirmed in CE<sub>B</sub> through limited proteolysis and N-terminal sequencing (data not shown) and is conserved in CE<sub>T</sub> and the neuronal *Drosophila* SCP2. GenBank accession nos. are AF322410 for CE<sub>B</sub>, U49390 for CE<sub>A</sub>, AAC28940 for CE<sub>T</sub>, AAB67805 for dSCP2, T30109 for F56D1.6, S13184 for ASCP III, AAB67804 and AE002777 (joined) for dSCP1, and T24726 for T09A5.1.

The sequence alignment of CE<sub>B</sub> with ASCP indicates that CE<sub>B</sub> has four putative EF-hand motifs, each motif containing a Ca<sup>2+</sup> binding loop and flanking  $\alpha$  helices. There is a high sequence similarity within the EF-hand motifs, with the exception of the fourth motif. This is due to the low sequence conservation of Ca<sup>2+</sup> coordinating residues Asp<sup>150</sup> (X), Leu<sup>152</sup> (Y), Asp<sup>154</sup> (Z), Gly<sup>156</sup> (-Y), Thr<sup>158</sup> (-X), and Thr<sup>161</sup> (-Z) in CE<sub>B</sub> (Fig. 1B). In a typical EF-hand the X position is Asp and the Z position is Asn, Asp, or Ser. The -Z position is always Asp or Glu, whereas the -Y position is rarely Gly, which may render the EF-hand non-functional (23, 24). The important hydrophobic residue between -Y and -X is lacking in CE<sub>B</sub> (Lys<sup>157</sup>; Fig. 1B). Based on this sequence alignment and the three-dimensional structure of ASCP (12), CE<sub>B</sub> most likely contains four helix-loop-helix structural elements, with the fourth EF-hand incapable of binding Ca<sup>2+</sup>. This contrasts with data for CE<sub>A</sub>, which was shown to bind only two Ca<sup>2+</sup>. This may be due to the condition used for the experiment, in which 5 mM MgCl<sub>2</sub> was present. SCPs have at least one Ca<sup>2+</sup>/Mg<sup>2+</sup> binding site (20); hence, one of the EF-hand sites in CE<sub>A</sub> may have been occupied with Mg<sup>2+</sup>.

GTP-binding proteins, including ARF (25), Ras protein (26), transducin (27), and elongation factor G (28), typically possess central  $\beta$  structures surrounded by  $\alpha$  helices (25–28). In all these proteins, the GTP binding site is defined by three sequence motifs in the strict order: GXXXXGK(S/T) ( $\Sigma$ 1), DXXG ( $\Sigma$ 2), and NKXD ( $\Sigma$ 3) (29). These motifs are completely conserved among all GTPases (30) and are referred to as the fingerprint of GTPase (31). In small GTPases, the  $\Sigma$ 1 and  $\Sigma$ 2 motifs are separated by about 40 residues and the  $\Sigma$ 2 and  $\Sigma$ 3 motifs by about 50–80 residues (31). Sequence similarity of

CEs to GTP-binding proteins is very low (*e.g.*, 11% amino acid identity to *D. melanogaster* ADP-ribosylation factor; Ref. 32). Despite this fact, Nelson *et al.* (4) reported that CE<sub>A</sub> contains GTP binding motifs, which are also present in CE<sub>B</sub>. However, in both CE<sub>A</sub> and CE<sub>B</sub>, only the putative  $\Sigma$ 2 GTP binding motif is fully conserved. The Lys residue in the  $\Sigma$ 3 motif is replaced with Ile and the first Gly residue in the  $\Sigma$ 1 motif is replaced with Thr (Fig. 1B). The order of the three motifs in the primary sequence of CE<sub>A</sub> and CE<sub>B</sub> ( $\Sigma$ 2,  $\Sigma$ 3, and  $\Sigma$ 1) also differs from that of all other small GTPases ( $\Sigma$ 1,  $\Sigma$ 2, and  $\Sigma$ 3) (29). Furthermore, the  $\Sigma$ 2 and  $\Sigma$ 3 motifs are separated by only a single residue (Fig. 1B), which is in disagreement with the motif spacing in small GTPases as presented above (31). Nevertheless, Nelson *et al.* (4) have shown that CE<sub>A</sub> binds GTP, although GTP binding occurred only in the absence of Mg<sup>2+</sup>. This Mg<sup>2+</sup> inhibition of GTP binding contrasts with structural studies of various GTPases in which Mg<sup>2+</sup> is critical in the coordination of the phosphate group of GTP (25–28).

Earlier studies on CE<sub>A</sub> (33) suggested that the protein forms a homodimer, most likely due to the formation of disulfide bonds between two CE<sub>A</sub> molecules via exposed Cys residues, in the absence of a reducing agent. Our *E. coli* expressed and purified CE<sub>B</sub> showed a single band of 23 kDa on SDS-PAGE (Fig. 2A). In addition, our analytical ultracentrifugation experiments showed that CE<sub>B</sub> is monomeric in both the presence and the absence of Ca<sup>2+</sup> (data not shown). This is consistent with earlier studies on SCPs, which are generally found as monomers, with the exception of crustacean and sandworm SCPs (20). In sandworm, Ca<sup>2+</sup> modulates dimerization (34), with no disulfide bond involvement (23). The Ca<sup>2+</sup> overlay blot of purified CE<sub>B</sub> (Fig. 2B) showed that the protein readily bound

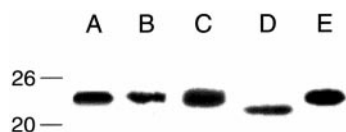


FIG. 2. A, SDS-PAGE of  $CE_B$ , showing a single band of about 23 kDa. B,  $^{45}Ca^{2+}$  overlay blot of  $CE_B$ . There is a single band of about 23 kDa. C, polyclonal  $CE_B$  antibody-stained Western blot of  $CE_B$ , showing a single band of about 23 kDa. The band disappeared when the antibodies were first incubated with  $CE_B$  (data not shown). D, polyclonal  $CE_B$  antibody-stained Western blot of squid optic lobe, showing a single band of about 22 kDa. The band disappeared when the antibodies were first incubated with  $CE_B$  (data not shown). E, protein kinase C phosphorylation of  $CE_B$ . There is a single band of about 23 kDa. Since PKC requires the presence of  $Ca^{2+}$ , only the  $Ca^{2+}$ -bound  $CE_B$  was used in this experiment. In contrast, although putative CKII phosphorylation consensus sequences are found in  $CE_B$ , CKII did not phosphorylate either  $Ca^{2+}$ -bound or  $Ca^{2+}$ -free  $CE_B$  (data not shown).

$^{45}Ca^{2+}$ . No extra band was seen, including that corresponding to a homodimer. A polyclonal antibody that was raised against the recombinant  $CE_B$  cross-reacted with a 23-kDa protein (Fig. 2C). The  $CE_B$  antibody also cross-reacted with a protein in the squid optic lobe (Fig. 2D). The single band found in the squid optic lobe ( $\sim 22$  kDa) is slightly smaller than the recombinant  $CE_B$ , which is probably due to the lack of the N-terminal addition of eight amino acids from the glutathione S-transferase fusion protein. When the antibody was preincubated with  $CE_B$  prior to incubation with the filter, no cross-reaction was observed on the Western blot either with  $CE_B$  or squid optic lobe tissue (data not shown), indicating that the antibodies are specific to  $CE_B$ .

It has been reported (4, 35) that  $CE_A$  is a high affinity substrate for PKC and has a single PKC phosphorylation site (Thr<sup>61</sup>). We found that  $CE_B$  was also a substrate for PKC in the presence of  $Ca^{2+}$  (Fig. 2E). There are two putative PKC phosphorylation sites in  $CE_B$  (Thr<sup>61</sup> and Thr<sup>188</sup>; Fig. 1B). Since  $CE_A$  possesses Thr<sup>61</sup> (4) but lacks Thr<sup>188</sup>, Thr<sup>61</sup> may be a common phosphorylation site in CEs. Our mass spectrometry data indicate that about 80% of the protein was phosphorylated at both Thr<sup>61</sup> and Thr<sup>188</sup> and the remaining 20% at one of the two sites. There is no detectable amount of unphosphorylated  $CE_B$  in the mass spectrum (data not shown). Whether or not the phosphorylation of these sites is functionally important remains unclear.

Previous far UV CD spectroscopy on  $CE_A$  (36) has shown that the  $Ca^{2+}$ -free protein is composed of 28%  $\alpha$  helix and 23%  $\beta$  sheet and the  $Ca^{2+}$ -bound protein is composed of 33%  $\alpha$  helix and 18%  $\beta$  sheet. However, as indicated above, the multiple sequence alignment suggested that  $CE_B$  is an  $\alpha$ -helical protein. In order to characterize the secondary structure of  $CE_B$ , we performed far UV CD spectroscopy (Fig. 3). Deconvolution of the CD data using a neural network algorithm (37) showed that  $Ca^{2+}$ -free  $CE_B$  contains 46%  $\alpha$  helix and 11%  $\beta$  sheet, whereas  $Ca^{2+}$ -bound  $CE_B$  contains 57%  $\alpha$  helix and 6%  $\beta$  sheet. Interestingly, the  $[\theta]_{208}$  value is more negative than the  $[\theta]_{222}$  value, atypical of the canonical  $\alpha$ -helical protein (38). Nevertheless, these data indicate that  $CE_B$  is highly  $\alpha$ -helical, consistent with the sequence analysis indicating that  $CE_B$  is an EF-hand protein. Hence, we believe that the content of  $\beta$  sheet reported for  $CE_A$  (36) and even those obtained for  $CE_B$  are overestimated. We also suggest that the difference in  $\alpha$  helix content between  $Ca^{2+}$ -free and  $Ca^{2+}$ -bound states may reflect changes in the orientation of preexisting  $\alpha$  helices upon  $Ca^{2+}$  binding (39). Nevertheless, the far UV CD data indicate that  $CE_B$  is folded even in the absence of  $Ca^{2+}$ .

The near UV CD spectrum of  $CE_B$  (Fig. 4) differs significantly between  $Ca^{2+}$ -free and  $Ca^{2+}$ -bound states, indicating that the protein undergoes a conformational change upon  $Ca^{2+}$

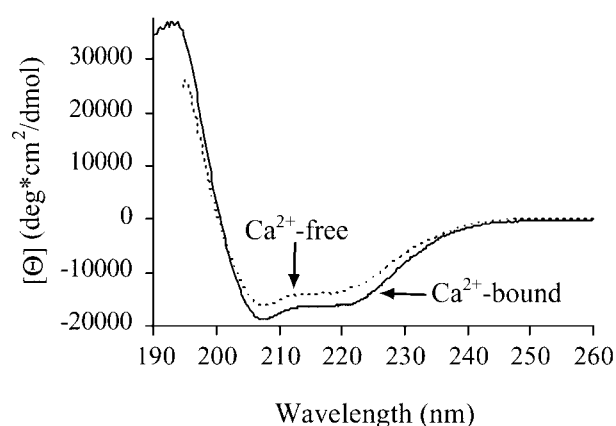


FIG. 3. Far UV circular dichroism spectra of  $Ca^{2+}$ -bound (solid line) and  $Ca^{2+}$ -free  $CE_B$  (dotted line). There is a spectral change upon addition of  $Ca^{2+}$ . Deconvolution of the data suggests that the  $Ca^{2+}$ -bound spectrum contains 57%  $\alpha$  helix and 6%  $\beta$  sheet. The  $Ca^{2+}$ -free spectrum is estimated to contain 46%  $\alpha$  helix and 11%  $\beta$  sheet. The  $[\theta]_{208}$  value is more negative than the  $[\theta]_{222}$  value, atypical of the canonical  $\alpha$ -helical protein (38), but consistent with other SCPs (56, 58–60).

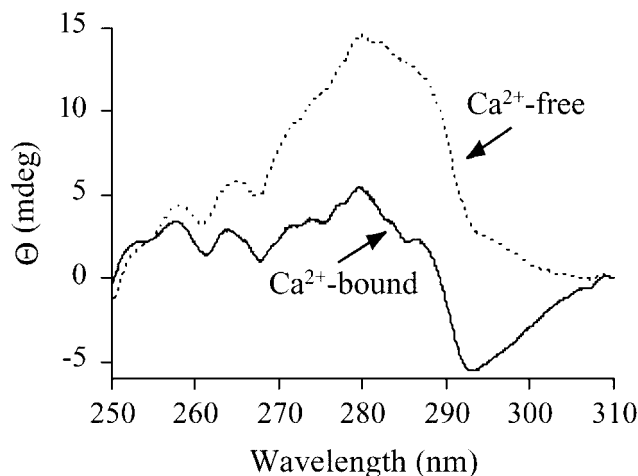
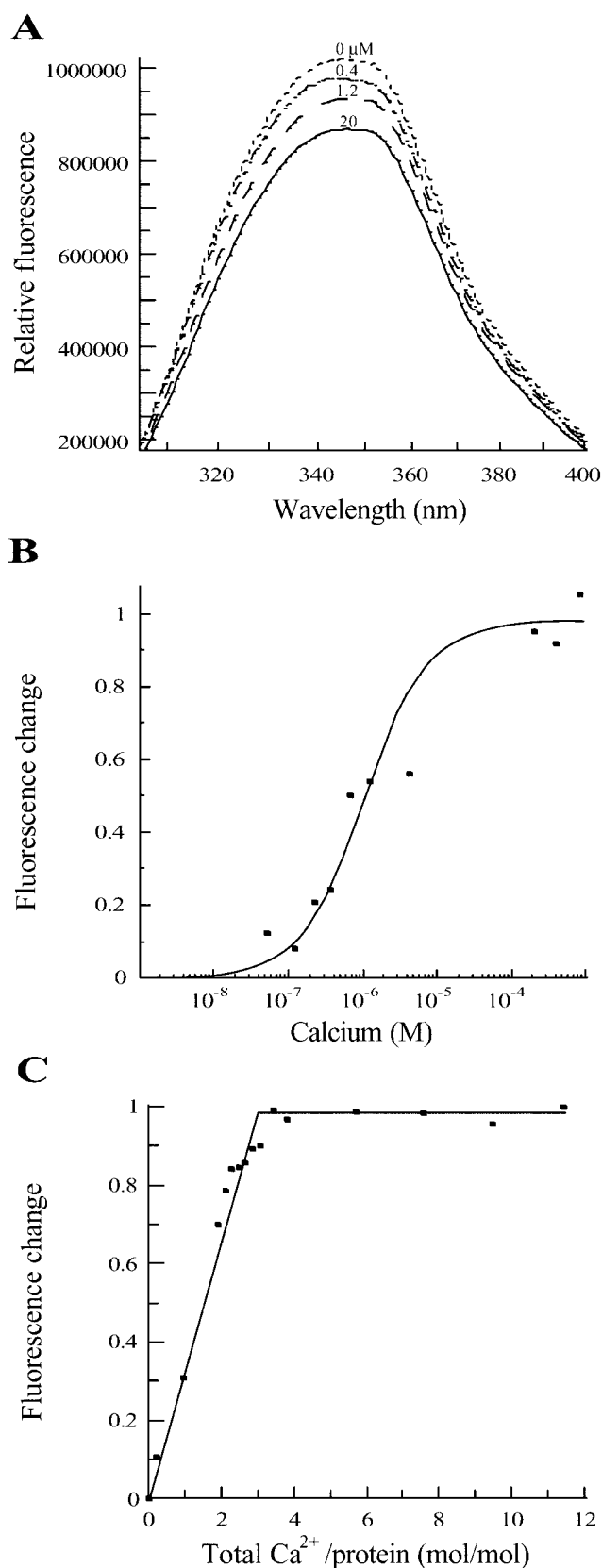


FIG. 4. Near UV circular dichroism spectra of  $Ca^{2+}$ -bound (solid line) and  $Ca^{2+}$ -free (dotted line)  $CE_B$ . There are approximately nine peaks in both  $Ca^{2+}$ -bound and  $Ca^{2+}$ -free  $CE_B$  spectra, due to an abundance of aromatic residues in the primary sequence. The spectrum indicates that the protein undergoes a  $Ca^{2+}$ -induced conformational change.

binding. In the region spanning 255 to 310 nm, there are approximately nine peaks in both  $Ca^{2+}$ -bound and  $Ca^{2+}$ -free  $CE_B$ , due to a number of aromatic residues (10 Phe, 7 Trp, and 7 Tyr) in  $CE_B$  (Fig. 1B). All nine peaks change in magnitude upon  $Ca^{2+}$  binding, suggesting that many of the aromatic residues undergo at least minor changes in their electronic environment. The largest change within this spectral region occurs between the wavelengths of 275 and 300 nm, corresponding to absorbance of Trp residues. Upon  $Ca^{2+}$  binding, the maximum at 280 nm decreases in signal intensity and a minimum at 293 nm becomes apparent, suggesting that Trp residues undergo a change in their environment. Contribution of Phe residues is also visible in the spectra. The minima at 261 and 267 nm are likely due to Phe residues. Minima at 263 and 268 nm are believed to be markers for the native fold (40). Furthermore, the existence of these minima suggests that at least some of the Phe residues are buried in specific and tightly packed environments (41).  $CE_B$  contains 10 Phe residues: four in the N-terminal half (residues 9, 18, 21, and 35) and six in the C-terminal half of the protein (residues 113, 115, 149, 165, 173, and 186; Fig. 1B). Residues 113, 165, 173, and 186 are well



**FIG. 5.  $\text{Ca}^{2+}$  binding measurements of  $\text{CE}_B$  using fluorescence spectroscopy.** A, tryptophan fluorescence emission spectra of  $\text{CE}_B$  at different  $\text{Ca}^{2+}$  concentrations. There is a 40% decrease in the fluorescence intensity upon  $\text{Ca}^{2+}$  binding, suggesting that  $\text{CE}_B$  undergoes a  $\text{Ca}^{2+}$ -induced conformational change involving the chemical environment of some, if not all, Trp residues. B, the change in fluorescence intensity integrated over the wavelength range of 305–400 nm is plotted as a function of free  $\text{Ca}^{2+}$  concentration. The binding curve indicates that the  $K_d$  of  $\text{CE}_B$  for  $\text{Ca}^{2+}$  is 1  $\mu\text{M}$ . C, the change in fluorescence

conserved among neuronal SCPs (Phe<sup>165</sup> is Lys in F56D1.6 and Phe<sup>186</sup> is Leu in  $\text{CE}_A$ , due to the shorter C terminus of  $\text{CE}_A$ ). In contrast, Phe residues 9, 18, 21, 35, 115, and 149 in  $\text{CE}_B$  are well conserved across both neuronal and muscle SCPs (residue 18 is Val and residue 21 is Met in dSCP1, and residue 149 is Tyr in ASCP). Furthermore, based on the three-dimensional structure of ASCP (12) and the multiple sequence alignment (Fig. 1B), the ASCP residues corresponding to the  $\text{CE}_B$  Phe residues 18, 21, 35, and 115 have solvent accessibilities of less than 3%. This suggests that these four Phe residues are part of the hydrophobic core of  $\text{CE}_B$  and contribute to the minima around 263 and 268 nm of the near UV CD spectra of  $\text{CE}_B$ .

$\text{CE}_B$  contains seven Trp residues: five in the N-terminal half (residues 32, 48, 66, 86, and 90) and two in the C-terminal half of the protein (residues 106 and 169). Most of these Trp residues are well conserved, and Trp<sup>66</sup> is completely conserved among the SCP proteins (Fig. 1B). As presented above, the near UV CD data indicated that the  $\text{Ca}^{2+}$ -induced conformational change of  $\text{CE}_B$  involves Trp residues. To confirm that the Trp residues undergo a change in their environment, we measured the change of fluorescence of Trp residues upon  $\text{Ca}^{2+}$  addition. The intrinsic fluorescence of the Trp indole ring showed a large decrease of fluorescence intensity (40%) upon  $\text{Ca}^{2+}$  addition (Fig. 5A). However, the change in the intensity was not accompanied by a significant shift of the maximum ( $\lambda_{\text{max}}$ ). This result is in agreement with the aforementioned near UV CD data (Fig. 4) and NMR data (see below). It is interesting to note that, in agreement with data presented above for Phe residues, Trp residues that are well conserved among SCPs (residues 66, 86, 90, and 106 in  $\text{CE}_B$ ) have low surface accessibilities (<7%) and hence are proposed to be part of the hydrophobic core of the proteins.

The change in fluorescence intensity plotted against  $\text{Ca}^{2+}$  concentration (Fig. 5B) shows that the midpoint of the titration occurs near 1  $\mu\text{M}$ . This value is comparable to the  $K_d$  of 0.4  $\mu\text{M}$  observed for  $\text{CE}_A$  (4) and is in the range expected for a  $\text{Ca}^{2+}$ -sensor protein (2). It is worth noting that the apparent  $K_d$  of  $\text{Ca}^{2+}$  binding to  $\text{CE}_B$  is larger than the  $K_d$  observed for  $\text{Ca}^{2+}$  binding to SCPs, which ranges from 0.1 to 0.01  $\mu\text{M}$  (42). Our experiments using tryptophan fluorescence spectroscopy show that  $\text{CE}_B$  binds three  $\text{Ca}^{2+}$  (Fig. 5C) in agreement with three conserved EF-hand  $\text{Ca}^{2+}$  binding loops, as described above. However, these data contrast with the previous report on  $\text{CE}_A$  (4), indicating that  $\text{CE}_A$  binds two  $\text{Ca}^{2+}$ . One possibility is that the presence of 5 mM  $\text{MgCl}_2$  in the  $\text{Ca}^{2+}$  binding study on  $\text{CE}_A$  may have contributed to this discrepancy. It has been known (42) that SCPs have  $\text{Ca}^{2+}/\text{Mg}^{2+}$  binding sites.

The effect of  $\text{Ca}^{2+}$  binding on  $\text{CE}_B$  was studied by NMR spectroscopy (Fig. 6, A and B). As seen in the  $^1\text{H}$ - $^{15}\text{N}$  HSQC spectrum of  $\text{Ca}^{2+}$ -free  $\text{CE}_B$  (Fig. 6B), most of the  $^{15}\text{N}$ -HN cross peaks are well dispersed, indicating that the protein is folded even without  $\text{Ca}^{2+}$ , in agreement with the far UV CD data presented above. The addition of  $\text{Ca}^{2+}$  resulted in a major spectral change, involving both chemical shift and intensity changes for a large fraction of cross peaks in the HSQC spectrum. In particular, the indole NH groups of several Trp residues in  $\text{CE}_B$ , resonating at >10 ppm (HN) and >130 ppm ( $^{15}\text{N}$ ), experience a large change in chemical shift upon the addition of  $\text{Ca}^{2+}$ , suggesting that most, if not all, Trp residues in  $\text{CE}_B$  change their chemical environment upon  $\text{Ca}^{2+}$  binding. This is in agreement with tryptophan fluorescence spectroscopy data

intensity integrated over the spectrum of 305 to 400 nm is plotted as a function of total  $\text{Ca}^{2+}$  concentration divided by the concentration of  $\text{CE}_B$ . The  $\text{Ca}^{2+}$  titration curve indicates that 3 mol of  $\text{Ca}^{2+}$  bind per mol of protein.



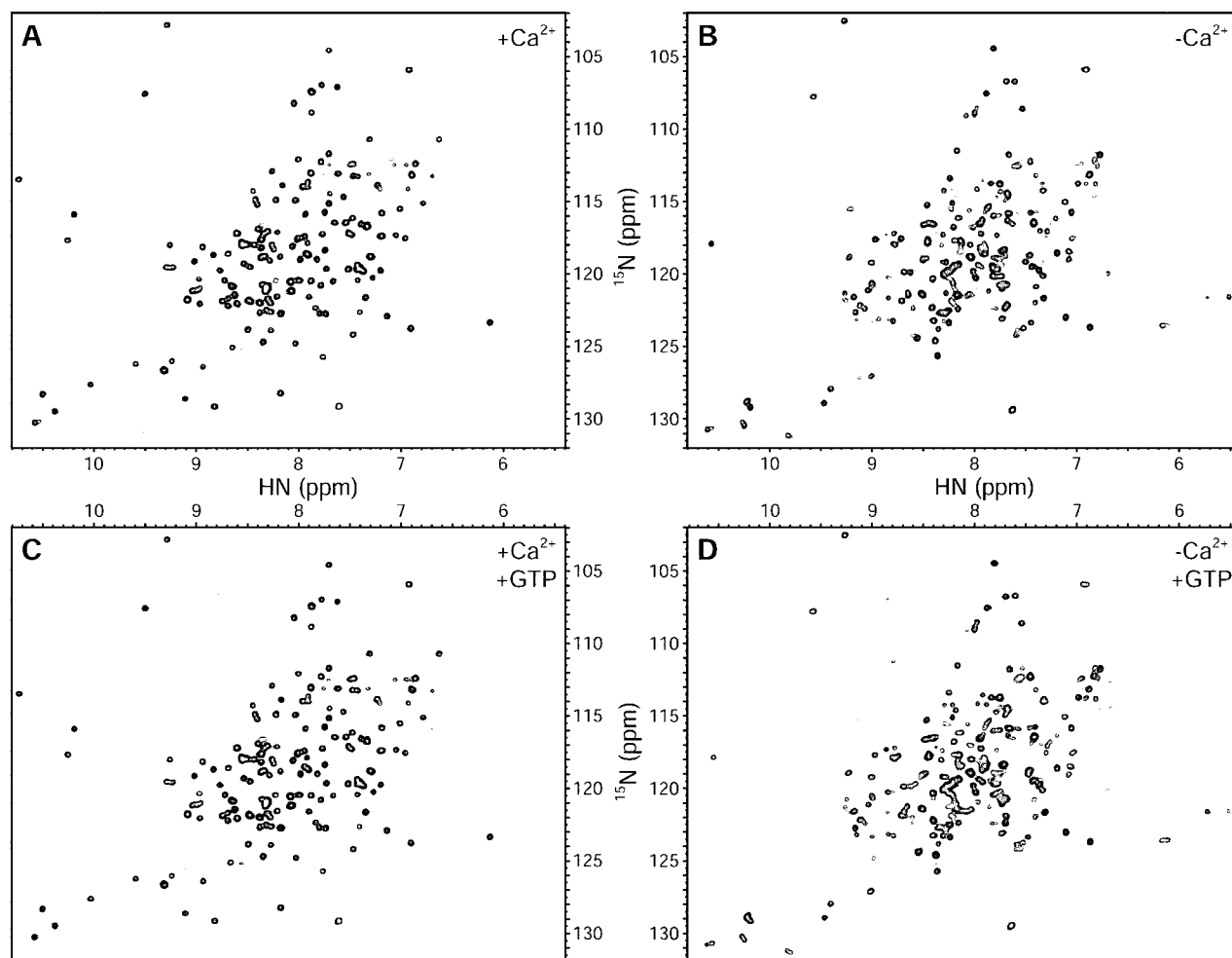


FIG. 6.  $^1\text{H}$ - $^{15}\text{N}$  HSQC spectra of  $\text{CE}_\text{B}$ . A,  $\text{CE}_\text{B}$  in the presence of 10 mM  $\text{CaCl}_2$  ( $\text{Ca}^{2+}$ -bound). The spectrum shows that the protein is folded since most peaks are well dispersed. B,  $\text{CE}_\text{B}$  in the presence of 10 mM EGTA ( $\text{Ca}^{2+}$ -free). When compared with the  $\text{Ca}^{2+}$ -bound  $\text{CE}_\text{B}$  spectrum, there is a change in chemical shift and intensity of a large fraction of cross peaks. The spectrum indicates that  $\text{CE}_\text{B}$  is folded even in the absence of  $\text{Ca}^{2+}$ . C,  $\text{CE}_\text{B}$  in the presence of 10 mM  $\text{CaCl}_2$  and 2 mM GTP. Since no spectral changes were visible upon the addition of GTP, this suggests that  $\text{CE}_\text{B}$  does not bind GTP. Furthermore, no spectral changes were observed even in the presence of 2 mM  $\text{MgCl}_2$  (data not shown), which is a critical ion for GTP binding (25–28). D,  $\text{CE}_\text{B}$  in the presence of 10 mM EGTA and 2 mM GTP. Only minor spectral changes were visible upon the addition of 2 mM  $\text{MgCl}_2$ , which were probably due to  $\text{Mg}^{2+}$  binding to the EF-hand(s). This suggests that, even in the absence of  $\text{Ca}^{2+}$ ,  $\text{CE}_\text{B}$  does not bind GTP.

discussed previously (Fig. 5). Interestingly, the spectrum of  $\text{Ca}^{2+}$ -free  $\text{CE}_\text{B}$  contains one downfield shifted peak (10.55 ppm (HN)/117.9 ppm ( $^{15}\text{N}$ )), whereas the spectrum of the  $\text{Ca}^{2+}$ -bound  $\text{CE}_\text{B}$  contains three downfield shifted peaks (10.73 (HN)/114.0 ppm ( $^{15}\text{N}$ ), 10.20 (HN)/116.5 ppm ( $^{15}\text{N}$ ), and 10.25 (HN)/118.2 ppm ( $^{15}\text{N}$ )). Peaks in this region are characteristic of the residue in the sixth position of the  $\text{Ca}^{2+}$  binding loop of the EF-hand domain, which is typically Gly (1, 24). The downfield shift of these residues are likely due to the hydrogen bond between the amide proton of the residue with the side chain of the Asp residue at the  $\text{Ca}^{2+}$  binding X position of the EF-hand domain (Fig. 1B) (43). It is worth noting that in  $\text{CE}_\text{B}$ , the Gly residue of EF2 is replaced by Glu and that of EF3 is replaced by Asn. In SCPs, the substitution of Gly to Asn or Glu does not interfere with  $\text{Ca}^{2+}$  binding (20, 42). To date,  $\text{CE}_\text{B}$  and SCP from *Nereis diversicolor* (44) are the only examples with HSQC spectra showing a large downfield shift of peaks (>2 ppm in the HN dimension) irrespective of residue type (Gly, Asn, and Glu in  $\text{CE}_\text{B}$ ; Gly and Asn in SCP from *N. diversicolor*) and corresponding to the sixth position of a functional  $\text{Ca}^{2+}$  binding loop. These NMR data are consistent with the tryptophan fluorescence data indicating that  $\text{CE}_\text{B}$  binds three  $\text{Ca}^{2+}$  ions. Furthermore, the NMR data also indicate that two hydrogen bonds are most likely broken in the  $\text{Ca}^{2+}$ -free state, since only one down-

field shifted peak remains in the spectrum of  $\text{Ca}^{2+}$ -free  $\text{CE}_\text{B}$ .

To test the binding of  $\text{Mg}^{2+}$  to  $\text{CE}_\text{B}$ , we recorded an HSQC spectrum of  $\text{CE}_\text{B}$  in the presence of 2 mM  $\text{Mg}^{2+}$ . The comparison of this spectrum with that of  $\text{Ca}^{2+}$ -free  $\text{CE}_\text{B}$  shows significant chemical shift changes for a number of peaks, indicating that  $\text{CE}_\text{B}$  binds  $\text{Mg}^{2+}$ . However, the changes are not as drastic as those observed when  $\text{Ca}^{2+}$  was added. For example, the two downfield shifted peaks that appear in the  $\text{Ca}^{2+}$ -bound  $\text{CE}_\text{B}$  spectrum (10.73 (HN)/114.0 ppm ( $^{15}\text{N}$ ) and 10.20 (HN)/116.5 ppm ( $^{15}\text{N}$ )) are not present in the  $\text{Mg}^{2+}$  spectrum (data not shown). A similar experiment was performed for  $\text{Ca}^{2+}$ -bound  $\text{CE}_\text{B}$ , in which no apparent change is detected upon addition of  $\text{Mg}^{2+}$  (data not shown), suggesting that the  $\text{Mg}^{2+}$  affinity of  $\text{CE}_\text{B}$  is lower than the  $\text{Ca}^{2+}$  affinity ( $K_d = 1 \mu\text{M}$ ).

In contrast to the drastic  $\text{Ca}^{2+}$ -induced change observed in the HSQC spectrum, the addition of GTP yielded only a negligible effect on the HSQC spectrum of  $\text{CE}_\text{B}$  (Fig. 6, C and D). Three independent GTP binding assays, nitrocellulose filtration (45), nitrocellulose overlay (46), and GTP cross-linking (47), did not reveal GTP binding to  $\text{CE}_\text{B}$  (data not shown). These observations and the poorly conserved GTP binding consensus sequences in  $\text{CE}_\text{B}$ , as discussed later, indicate that  $\text{CE}_\text{B}$  lacks GTP binding activity.

## DISCUSSION

The SCP protein subfamily of the EF-hand superfamily comprises a number of invertebrate muscle proteins, with molecular masses ranging from 20 to 22 kDa. However, there have been reports that describe SCP proteins existing in neuronal tissue (21, 48). In *Helix pomatia* (49) and in *Aplysia californica* (48), a terrestrial and a marine invertebrate, respectively, there is immunohistochemical evidence that SCPs are found in neuronal cells. Furthermore, in *D. melanogaster*, the gene sequences of an SCP protein from the muscle and another from the nervous tissue have been identified (with the proteins sharing only 19% identity), with no spatial overlap in expression (21). Taken together, these data suggest that a neuronal counterpart of SCP proteins may exist in invertebrates, although only a muscle isoform has been identified in the majority of organisms. It is worth mentioning that, in *D. melanogaster*, for which the complete genome is known (50), there is no evidence for protein isoforms, which is in agreement with a study reported previously (21).

The multiple sequence alignment also reveals that neuronal SCP proteins share a fingerprint "YXNFM" motif in the entering EF3  $\alpha$  helix (Fig. 1B). Based on the multiple sequence alignment and the conservation of the fingerprint region in the EF3 motif, we propose that the putative *C. elegans* F56D1.6 protein is a neuronal SCP protein. The lack of the neuronal motif in the putative *C. elegans* protein T09A5.1 suggests that this protein is a muscle SCP protein. The muscle and neuronal proteins in *C. elegans* are only 26% identical. These data are in agreement with those in *D. melanogaster*, suggesting that, even in the same organism, muscle and neuronal SCPs are very different. Furthermore, there is no supporting evidence for SCP isomers (other than the neuronal and muscle homologues mentioned above) in the known genome of *C. elegans* (22), which is in agreement with the *D. melanogaster* data discussed previously. Nevertheless, all these data suggest that SCP proteins can be subdivided into two classes based on tissue distribution and/or primary sequence. SCPs have been thought to act as  $\text{Ca}^{2+}$  buffers (42), since SCPs were found to be highly concentrated in invertebrate muscles, possessed  $\text{Ca}^{2+}/\text{Mg}^{2+}$  binding sites, and no target protein was identified (20). To this end, it is worthwhile to point out that CE is the first example of an SCP family member that functions as a  $\text{Ca}^{2+}$  sensor. It is tempting to speculate that only neuronal SCPs acquired  $\text{Ca}^{2+}$  sensor function, whereas muscle SCPs function as  $\text{Ca}^{2+}$  buffers. Clearly, further investigation is required to address this hypothesis.

It has been postulated that  $\text{CE}_A$  is a membrane-binding protein (4, 33, 51, 52), because of the 3' terminal polyisoprenylation consensus domain (CAAX) and two putative myristoylation consensus sequences (4). Interestingly, the polyisoprenylation signaling sequence is absent in  $\text{CE}_B$ , whereas two myristoylation consensus sequences are present in  $\text{CE}_B$ . However, myristoylation can only occur at the N terminus of a mature protein (53, 54). Taken together, we believe that  $\text{CE}_B$  is a cytoplasmic protein, like other SCPs (20).

PKC plays a pivotal role in activity-dependent neuronal plasticity with various pathways (55). Although PKC phosphorylates  $\text{CE}_B$  (Fig. 2B), the lack of conservation of PKC phosphorylation sites even among neuronal SCPs suggests that PKC phosphorylation may not be essential for CEs. Furthermore, PKC phosphorylation failed to produce any detectable global changes in the conformation of  $\text{CE}_B$  using CD or fluorescence spectroscopy (data not shown).  $\text{CE}_B$  also has four putative CKII phosphorylation sites, one of which is located in the EF2 loop and conserved among all SCP homologues presented in Fig. 1B. However, CKII failed to phosphorylate either

the  $\text{Ca}^{2+}$ -bound or  $\text{Ca}^{2+}$ -free  $\text{CE}_B$  (data not shown), in agreement with the previous study of  $\text{CE}_A$  (4).

$\text{CE}_B$  binds  $\text{Ca}^{2+}$ , which leads to major conformational changes as monitored by far and near UV CD spectroscopy, fluorescence spectroscopy, and NMR spectroscopy. The far UV CD spectrum of  $\text{CE}_B$  (Fig. 3) is nearly identical to that reported for  $\text{CE}_A$  (36). The spectra of  $\text{CE}_B$  also show a remarkable similarity to the spectra observed with other SCPs: a high  $[\Theta]_{222}$  (56–60), which is probably due to the contribution of aromatic residues flanking the  $\alpha$  helices (61).

Near UV CD data showed that the protein undergoes a conformational change upon  $\text{Ca}^{2+}$  addition, since there are spectral changes between 255 and 310 nm (Fig. 4). These data are in agreement with previous results for SCP from *N. diversicolor*, which showed that the spectrum between 255 and 300 nm changed dramatically with the addition of  $\text{Ca}^{2+}$  (34, 56). Similar changes have been observed in other EF-hand CaBPs such as S100P (62). Furthermore, near UV CD data suggest that both  $\text{Ca}^{2+}$ -free and  $\text{Ca}^{2+}$ -bound  $\text{CE}_B$  is in a native-like conformation, due to characteristic minima around 263 and 268 nm (40).

The intrinsic tryptophan fluorescence data, in agreement with the near UV CD data presented above, indicate that Trp residues are involved in the  $\text{Ca}^{2+}$ -induced conformational change in  $\text{CE}_B$ . The fluorescence spectral change comprises a reduction in intensity with no significant shift of  $\lambda_{\text{max}}$ . Similar spectral change has been observed for other EF-hand CaBPs, such as scallop SCP (57), frequenin (63), neurocalcin  $\alpha$  and  $\beta$  (64), S100P (62), and parvalbumin (65). The change in intensity of the signal combined with a lack of shift of  $\lambda_{\text{max}}$  has been suggested to occur due to a change in the electronic environment of Trp residues (65). Interestingly, the signal intensity has decreased in three of the aforementioned CaBPs upon  $\text{Ca}^{2+}$  binding. In SCP,  $\text{Ca}^{2+}$  binding resulted in a signal intensity decrease of 80% (57), in frequenin a decrease of 25% (63), and in S100P a decrease of 20% (62).

As indicated by tryptophan fluorescence spectroscopy, NMR spectroscopy suggests that Trp residues change their chemical environment upon  $\text{Ca}^{2+}$  binding. In contrast to tryptophan fluorescence spectroscopy, which provides information of the global changes of Trp side chains, NMR spectroscopy provides detailed information of individual Trp indole rings. However, the interpretation of the HSQC spectra is limited by the lack of resonance assignments. Nevertheless,  $^{15}\text{N}$ -HN cross peaks resonating at  $>10$  ppm (HN) and  $>130$  ppm ( $^{15}\text{N}$ ) are likely due to the indole NH groups of Trp residues. All of these Trp peaks experience a chemical shift change upon  $\text{Ca}^{2+}$  binding, suggesting that these Trp residues undergo changes in their chemical environment.

The  $\text{Ca}^{2+}$ -induced NMR spectral changes of the Trp indole rings are also accompanied by major changes in the rest of the spectrum. This may indicate that  $\text{Ca}^{2+}$  binding induces a gross conformational change that extends to the entire molecule. Although GTP binding has been previously reported for  $\text{CE}_A$  (4), based on NMR spectroscopy and binding assays we found no evidence for GTP binding to  $\text{CE}_B$ . Our NMR data indicate that the  $K_d$  for GTP binding to  $\text{CE}_B$ , if any, is larger than 2 mM. This is significantly larger than the  $K_d$  for specific GTP binding to other small GTPases, which ranges from 0.05 to 5  $\mu\text{M}$  (66). Therefore, we conclude that  $\text{CE}_B$  is not a GTP-binding protein.

In conclusion,  $\text{CE}_B$  is a member of the SCP subfamily of the EF-hand superfamily, belonging to the neuronal type.  $\text{CE}_B$  binds three  $\text{Ca}^{2+}$  ions with an apparent  $K_d$  of 1  $\mu\text{M}$ . There is a conformational change induced by  $\text{Ca}^{2+}$ , which (based on optical and NMR spectroscopies) also involves a change in the environment of many aromatic residues. Our data indicate that

CE<sub>B</sub> is not a GTP-binding protein, and thus it is not a GTPase. The protein is a substrate of PKC, although this may be physiologically irrelevant.

At present, it is unclear what the biological significance of neuronal SCP isoforms may be, especially since in *Drosophila* there are no SCP isoforms in either muscle or neurons (21, 50). One possibility may be to provide a "fine-tuning" mechanism in the action of CE. Detailed structural and physiological studies will be necessary to identify the mechanism(s) of action of CE<sub>B</sub>.

**Acknowledgments**—We thank Dr. J. B. Ames and Dr. M. B. Swindells for discussions, Dr. R. Ishima and Dr. D. Liu for help with NMR, K. Tong with laboratory help, and Dr. D. L. Alkon and Dr. T. J. Nelson with initial help with the work.

## REFERENCES

- Kretsinger, R. H., and Nockolds, C. E. (1973) *J. Biol. Chem.* **248**, 3313–3326
- Ikura, M. (1996) *Trends Biochem. Sci.* **21**, 14–17
- Nelson, T. J., Collin, C., and Alkon, D. L. (1990) *Science* **247**, 1479–1483
- Nelson, T. J., Cavallaro, S., Yi, C. L., McPhie, D., Schreurs, B. G., Gusev, P. A., Favit, A., Zohar, O., Kim, J., Beushausen, S., Ascoli, G., Olds, J., Neve, R., and Alkon, D. L. (1996) *Proc. Natl. Acad. Sci. U. S. A.* **93**, 13808–13813
- Alkon, D. L., Nelson, T. J., Zhao, W., and Cavallaro, S. (1998) *Trends Neurosci.* **21**, 529–537
- Nelson, T. J., Zhao, W. Q., Yuan, S., Favit, A., Pozzo-Miller, L., and Alkon, D. L. (1999) *Biochem. J.* **341**, 423–433
- Cavallaro, S., Meiri, N., Yi, C. L., Musco, S., Ma, W., Goldberg, J., and Alkon, D. L. (1997) *Proc. Natl. Acad. Sci. U. S. A.* **94**, 9669–9673
- Kim, C. S., Han, Y. F., Etcheberrygaray, R., Nelson, T. J., Olds, J. L., Yoshioka, T., and Alkon, D. L. (1995) *Proc. Natl. Acad. Sci. U. S. A.* **92**, 3060–3064
- Etcheberrygaray, E., Gibson, G. E., and Alkon, D. L. (1994) *Ann. N. Y. Acad. Sci.* **747**, 245–255
- Sun, M. K., Nelson, T. J., Xu, H., and Alkon, D. L. (1999) *Proc. Natl. Acad. Sci. U. S. A.* **96**, 7023–7028
- Thompson, J. D., Gibson, T. J., Plewniak, F., Jeanmougin, F., and Higgins, D. G. (1997) *Nucleic Acids Res.* **25**, 4876–4882
- Cook, W. J., Jeffrey, L. C., Cox, J. A., and Vijay-Kumar, S. (1993) *J. Mol. Biol.* **229**, 461–471
- Sambrook, J., Fritsch, E. F., and Maniatis, T. (1989) *Molecular Cloning: A Laboratory Manual*, 2nd Ed., Cold Spring Harbor Laboratory Press, Cold Spring Harbor, NY
- Campbell, J. A., Biggart, J. D., and Elliott, R. J. (1991) *Biochem. Soc. Trans.* **19**, 53S
- Gill, S. C., and von Hippel, P. H. (1989) *Anal. Biochem.* **182**, 319–326
- Bodenhausen, G., and Ruben, D. J. (1979) *Chem. Phys. Lett.* **69**, 185–189
- Zhang, O., Kay, L. E., Olivier, J. P., and Forman-Kay, J. D. (1994) *J. Biomol. NMR* **4**, 845–858
- Kay, L. E., Keifer, P., and Saarinen, T. (1992) *J. Magn. Reson. A* **109**, 129–133
- Takagi, T., and Cox, J. A. (1990) *Eur. J. Biochem.* **192**, 387–399
- Cox, J. A., Luan-Rilliet, Y., and Takagi, T. (1991) in *Novel Calcium-binding Proteins: Fundamentals and Clinical Implications* (Heizmann, C. W., ed) pp. 447–463, Springer-Verlag, New York
- Kelly, L. E., Phillips, A. M., Delbridge, M., and Stewart, R. (1997) *Insect Biochem. Mol. Biol.* **27**, 783–792
- The *C. elegans* Sequencing Consortium (1998) *Science* **282**, 2012–2018
- Vijay-Kumar, S., and Cook, W. J. (1992) *J. Mol. Biol.* **224**, 413–426
- Kawasaki, H., and Kretsinger, R. H. (1994) *Protein Profile* **1**, 343–517
- Greasley, S. E., Jhota, H., Teahan, C., Solari, R., Fensome, A., Thomas, G. M., Cockcroft, S., and Bax, B. (1995) *Nat. Struct. Biol.* **2**, 797–806
- de Vos, A. M., Tong, L., Milburn, M. V., Matias, P. M., Jancarik, J., Noguchi, S., Nishimura, S., Miura, K., Ohtsuka, E., and Kim, S. H. (1988) *Science* **239**, 888–893
- Lambright, D. G., Noel, J. P., Hamm, H. E., and Sigler, P. B. (1994) *Nature* **369**, 621–628
- Czworkowski, J., Wang, J., Steitz, T. A., and Moore, P. B. (1994) *EMBO J.* **13**, 3661–3668
- Kjeldgaard, M., Nyborg, J., and Clark, B. F. (1996) *FASEB J.* **10**, 1347–1368
- Cuvillier, A., Redon, F., Antoine, J., Chardin, P., DeVos, T., and Merlin, G. (2000) *J. Cell Sci.* **113**, 2065–2074
- Dever, T. E., Glynnias, M. J., and Merrick, W. C. (1987) *Proc. Natl. Acad. Sci. U. S. A.* **84**, 1814–1818
- Tamkun, J. W., Kahn, R. A., Kissinger, M., Brizuela, B. J., Rulka, C., Scott, M. P., and Kennison, J. A. (1991) *Proc. Natl. Acad. Sci. U. S. A.* **88**, 3120–3134
- Nelson, T. J., Yoshioka, T., Toyoshima, S., Han, Y. F., and Alkon, D. L. (1994) *Proc. Natl. Acad. Sci. U. S. A.* **91**, 9287–9291
- Durussel, I., Luan-Rilliet, Y., Petrova, T., Takagi, T., and Cox, J. A. (1993) *Biochemistry* **32**, 2394–2400
- Nelson, T. J., and Alkon, D. L. (1995) *J. Neurochem.* **65**, 2350–2357
- Ascoli, G. A., Luu, K. X., Olds, J. L., Nelson, T. J., Gusev, P. A., Bertucci, C., Bramanti, E., Raffaelli, A., Salvadori, P., and Alkon, D. L. (1997) *J. Biol. Chem.* **272**, 24771–24779
- Greenfield, N. J. (1996) *Anal. Biochem.* **235**, 1–10
- Chen, Y. H., Yang, J. T., and Chau, K. H. (1974) *Biochemistry* **13**, 3350–3359
- Williams, T. C., Corson, D. C., Oikawa, K., McCubbin, W. D., Kay, C. M., and Sykes, B. D. (1986) *Biochemistry* **25**, 1835–1846
- Pain, R. (1996) in *Current Protocols in Protein Science* (Coligan, J. E., Dunn, B., Ploegh, H. L., Speicher, D. W., Wingfield, P. T., eds) pp. 761–823, John Wiley & Sons, Toronto
- Strickland, E. H. (1974) *CRC Crit. Rev. Biochem.* **2**, 113–175
- Hermann, A., and Cox, J. A. (1991) *Comp. Biochem. Physiol.* **111B**, 337–345
- Ikura, M., Minowa, O., and Hikichi, K. (1985) *Biochemistry* **24**, 4264–4269
- Craescu, C. T., Precheur, B., van Riel, A., Sakamoto, H., Cox, J. A., and Engelborghs, Y. (1998) *J. Biomol. NMR* **12**, 565–566
- Mitchell, J., and Mayeenuddin, L. H. (1998) *Biochemistry* **37**, 9064–9072
- Manser, E., Leung, T., and Lim, L. (1995) *Methods Enzymol.* **256**, 130–139
- Tanaka, T., Saha, S. K., Tomomori, C., Ishima, R., Liu, D., Tong, K. I., Park, H., Dutta, R., Qin, L., Swindells, M. B., Yamazaki, T., Ono, A. M., Kainosho, M., Inouye, M., and Ikura, M. (1998) *Nature* **396**, 88–92
- Pauls, T. L., Cox, J. A., Heizmann, C. W., and Hermann, A. (1993) *Eur. J. Neurosci.* **5**, 549–559
- Kerschbaum, H. H., Kainz, V., and Hermann, A. (1992) *Brain Res.* **597**, 339–342
- Adams, M. D., Celniker, S. E., Holt, R. A., Evans, C. A., Gocayne, J. D., Amanatides, P. G., Scherer, S. E., Li, P. W., Hoskins, R. A., Galle, R. F., George, R. A., Lewis, S. E., Richards, S., Ashburner, M., Henderson, S. N., Sutton, G. G., Wortman, J. R., Yandell, M. D., Zhang, Q., Chen, L. X., Brandon, R. C., Rogers, Y. H., Blazej, R. G., Champe, M., Pfeiffer, B. D., Wan, K. H., Doyle, C., Baxter, E. G., Helt, G., Nelson, C. R., Gabor Miklos, G. L., Abril, J. F., Agbayani, A., An, H. J., Andrews-Pfannkoch, C., Baldwin, D., Ballew, R. M., Basu, A., Baxendale, J., Bayraktaroglu, L., Beasley, E. M., Beeson, K. Y., Benos, P. V., Berman, B. P., Bhandari, D., Bolshakov, S., Borkova, D., Botchan, M. R., Bouck, J., Brokstein, P., Brottier, P., Burtis, K. C., Busam, D. A., Butler, H., Cadieu, E., Center, A. C., Chandra, L., Cherry, J. M., Cawley, S., Dahlke, C., Davenport, L. B., Davies, P., de Pablos, B., Delcher, A., Deng, Z., Mays, A. D., Dew, I., Dietz, S. M., Dodson, K., Doup, L. E., Downes, M., Dugan-Rocha, S., Dunkov, B. C., Dunn, P., Durbin, K. J., Evangelista, C. C., Ferraz, C., Ferriera, S., Fleischmann, W., Fosler, C., Gabrieli, A. E., Garg, N. S., Gelbart, W. M., Glasser, K., Glodek, A., Gong, F., Gorrell, J. H., Gu, Z., Guan, P., Harris, M., Harris, N. L., Harvey, D., Heiman, T. J., Hernandez, J. R., Houck, J., Hostin, D., Houston, K. A., Howland, T. J., Wei, M. H., Ibegwam, C., Jalali, M., Kalush, F., Karpen, G. H., Ke, Z., Kennison, J. A., Ketchum, K. A., Kimmel, B. E., Kodira, C. D., Kraft, C., Kravitz, S., Kulp, D., Lai, Z., Lasko, P., Lei, Y., Levitsky, A. A., Li, J., Li, Z., Liang, Y., Lin, X., Liu, X., Mattei, B., McIntosh, T. C., McLeod, M. P., McPherson, D., Merkulov, G., Milshina, N. V., Mobarry, C., Morris, J., Moshrefi, A., Mount, S. M., Moy, M., Murphy, B., Murphy, L., Muzny, D. M., Nelson, D. L., Nelson, D. R., Nelson, K. A., Nixon, K., Nusser, D. R., Pauley, J. M., Palazzolo, M., Pittman, G. S., Pan, S., Pan, S., Pollard, J., Puri, V., Reese, M. G., Reinert, K., Remington, K., Saunders, R. D., Scheeler, F., Shen, H., Shue, B. C., Siden-Kiamos, I., Simpson, M., Skupski, M. P., Smith, T., Spier, E., Spradling, A. C., Stapleton, M., Strong, R., Sun, E., Svirskas, R., Tector, C., Turner, R., Venter, E., Wang, A. H., Wang, X., Wang, Z. Y., Wassarman, D. A., Weinstock, G. M., Weissbach, J., Williams, S. M., Woodage, T., Worley, K. C., Wu, D., Yang, S., Yao, Q. A., Ye, J., Yeh, R. F., Zaveri, J. S., Zhan, M., Zhang, G., Zhao, Q., Zheng, L., Zheng, X. H., Zhong, F. N., Zhong, W., Zhou, X., Zhu, S., Zhu, X., Smith, H. O., Gibbs, R. A., Myers, E. W., Rubin, G. M., and Venter, J. C. (2000) *Science* **287**, 2185–2195
- Nelson, T. J., Sanchez-Andres, J. V., Schreurs, B. G., and Alkon, D. L. (1991) *J. Neurochem.* **57**, 2065–2069
- Kuzirian, A. M., Epstein, H. T., Nelson, T. J., Rafferty, N. S., and Alkon, D. L. (1998) *Biol. Bull.* **195**, 198–201
- Grand, R. J. (1989) *Biochem. J.* **258**, 625–638
- Ames, J. B., Ishima, R., Tanaka, T., Gordon, J. I., Stryer, L., and Ikura, M. (1997) *Nature* **389**, 198–202
- Tanaka, C., and Nishizuka, Y. (1994) *Annu. Rev. Neurosci.* **17**, 551–567
- Cox, J. A., Kretsinger, R. H., and Stein, E. A. (1981) *Biochim. Biophys. Acta* **670**, 441–444
- Collins, J. H., Johnson, J. D., and Szent-Gyorgyi, A. G. (1983) *Biochemistry* **22**, 341–345
- Cox, J. A., Winge, D. R., and Stein, E. A. (1979) *Biochimie (Paris)* **61**, 601–605
- Kohler, L., Cox, J. A., and Stein, E. A. (1978) *Mol. Cell. Biochem.* **20**, 85–93
- Closset, J., and Gerday, C. (1975) *Biochim. Biophys. Acta* **405**, 228–235
- Chakrabarty, A., Kortemme, T., Padmanabhan, S., and Baldwin, R. L. (1993) *Biochemistry* **32**, 5560–5565
- Gribenko, A., Lopez, M. M., Richardson, J. M., III, and Makhatadze, G. I. (1998) *Protein Sci.* **7**, 211–215
- Ames, J. B., Hendricks, K. B., Strahl, T., Huttner, I. G., Hamasaki, N., and Thorner, J. (2000) *Biochemistry* **39**, 12149–12161
- Kato, M., Watanabe, Y., Iino, S., Takaoka, Y., Kobayashi, S., Haga, T., and Hidaka, H. (1998) *Biochem. J.* **331**, 871–876
- Pauls, T. L., Durussel, I., Cox, J. A., Clark, I. D., Szabo, A. G., Gagne, S. M., Sykes, B. D., and Berchtold, M. W. (1993) *J. Biol. Chem.* **268**, 20897–20903
- Bobak, D. A., Bliziotis, M. M., Noda, M., Tsai, S. C., Adamik, R., and Moss, J. (1990) *Biochemistry* **29**, 855–861